Smart Structures and Systems, *Vol. 15, No. 2 (2015) 259-281*
DOI: http://dx.doi.org/10.12989/sss.2015.15.2.259

Structural identification of gravity-type caisson structure via vibration feature analysis

So-Young Lee[a], Thanh-Canh Huynh[b] and Jeong-Tae Kim*

Department of Ocean Engineering, Pukyong National University, Busan 608-737, Korea

(Received October 9, 2014, Revised January 13, 2015, Accepted January 16, 2015)

Abstract. In this study, a structural identification method is proposed to assess the integrity of gravity-type caisson structures by analyzing vibration features. To achieve the objective, the following approaches are implemented. Firstly, a simplified structural model with a few degrees-of-freedom (DOFs) is formulated to represent the gravity-type caisson structure that corresponds to the sensors' DOFs. Secondly, a structural identification algorithm based on the use of vibration characteristics of the limited DOFs is formulated to fine-tune stiffness and damping parameters of the structural model. Finally, experimental evaluation is performed on a lab-scaled gravity-type caisson structure in a 2-D wave flume. For three structural states including an undamaged reference, a water-level change case, and a foundation-damage case, their corresponding structural integrities are assessed by identifying structural parameters of the three states by fine-tuning frequency response functions, natural frequencies and damping factors.

Keywords: structural identification; gravity-type caisson; simplified vibration model; wave flume; stiffness; damping, modal parameters

1. Introduction

Over the last two decades, many gravity-type caisson structures have been constructed in Korea for the use of breakwater and quay wall. Caisson structures stand on foundation mound constructed above seabed and stabilized by their own weights. Most body of harbor caisson is submerged in sea water to keep the tranquility in harbor by dissipating wave energy from open sea. The caisson structures cannot be ensured for its safety upon repeatedly experiencing wave forces that are stronger than design wave forces. Due to the severe loading conditions, those structures may result in systematic changes deviated from the as-built designs.

Recent years, the integrity of harbor caisson structures becomes more important issue due to severe environmental phenomena and extreme events like large-scale typhoon or ship collision. For instance, typhoon Maemi hit the southern part of the Korean Peninsula in 2003 and it resulted in failure of gravity-type caisson structures. The gravity-type caisson structure is inevitably damaged due to local failures or global instability problems which are mostly attributed to

*Corresponding author, Professor, E-mail: idis@pknu.ac.kr
[a] Research Assistant
[b] Graduate Student

http://www.techno-press.org/?journal=sss&subpage=8 ISSN: 1738-1584 (Print), 1738-1991 (Online)

problems in foundation-structure interface. For instance, upon experiencing extreme wave forces, local defects such as cavity and displacement occurred in the foundation mound are eventually transformed into structural instable states by weakening global functionality against settlement, overturning and sliding of the structure (Oumeraci 1994, Goda 1994, Takahashi *et al*. 2000, Lee *et al*. 2009). Therefore, there is a need to identify the structural performance of the damaged caisson system which is locally defected in the foundation-structure interface.

Many researchers have worked on the so-called vibration-based structural health monitoring techniques, which implement vibration characteristics for structural integrity assessment, in the field of civil engineering (Adams *et al*. 1978, Stubbs and Osegueda 1990, Li *et al*. 2004, Jang *et al*. 2012, Huang and Nargarajaiah 2014, You *et al*. 2014). Also, many researchers have worked on developing structural identification methods such as modal sensitivity method, modal flexibility method, genetic algorithm, neural network, etc. (Aktan *et al*. 1997, Kim *et al*. 2003, Yun *et al*. 2009, Li *et al*. 2014, Gul *et al*. 2014). Despite those research efforts, coastal and harbor caisson structures have been treated by only a few research attempts, which include vibration response analyses and structural integrity estimation (Yang *et al*. 2001, Kim *et al*. 2005, Lee *et al*. 2013, Yi *et al*. 2013).

For the vibration-based structural health monitoring of gravity-type caisson structures, at least a few research needs exist. There are needs to experimentally analyze their vibration characteristics via the limited accessibility and to estimate their structural integrities by using changes in the vibration characteristics (Lee *et al*. 2013, Le *et al*. 2013). Related to these research needs, this study has been motivated to resolve three important issues: the first one is to construct a simplified structural model which can represent the caisson structural system with limited degrees-of-freedom (DOFs) adopted for vibration measurement; the second one is to estimate structural integrity of the caisson system via the simplified structural model; and the third one is to examine effects of water-level change and foundation damage on the structural integrity of the caisson system.

In this study, a structural identification method is proposed to assess the integrity of gravity-type caisson structures by analyzing vibration features. To achieve the objective, the following approaches are implemented. Firstly, a simplified structural model with a few DOFs is formulated to represent the gravity-type caisson structure that corresponds to the sensors' DOFs. Secondly, a structural identification algorithm based on the use of vibration characteristics of the limited DOFs is formulated to fine-tune the structural model. Structural stiffness and damping are selected as two key parameters to be identified for the model update. Finally, experimental evaluation is performed on a lab-scaled gravity-type caisson system in a 2-D wave flume. Three test scenarios are selected as an undamaged reference, a water-level change state, and a foundation-damage state. For each case, the corresponding structural integrity is assessed by identifying its structural parameters by fine-tuning frequency response functions, natural frequencies and damping factors.

2. Simplified structural model of gravity-type caisson system

Since as early as 1990, many researchers have worked on structural modeling of caisson structural systems (Smirnov and Moroz 1983, Marinski and Oumeraci 1992, Goda 1994, Oumeraci and Kortenhaus 1994, Vink 1997, Zhang 2006, Wang *et al*. 2006). However, the proposed models would not fit into the usage for structural identification because most of them require certain DOFs to be guaranteed for the function of the models. In another words, the limitation in measurable DOFs of in-field caisson systems, which is mainly due to the lack of accessibility, hinders the model's usage for structural integrity assessment. Moreover, the modeling becomes complicated as it deals with interlocking conditions since it requires additional DOFs of vibration responses.

In order to overcome the above-mentioned limitations, in this study, a simplified structural model is formulated to represent the gravity-type caisson structure with a few DOFs that correspond to the sensors' DOFs. It is noted that this study is limited to a planar model of a system of three interlocked caissons on the basis of the existing models proposed by Goda (1994), Oumeraci and Kortenhaus (1994), and Vink (1997). As shown in Fig. 1(a), the caisson system is subjected to an impulsive breaking wave force that results in forced vibration responses. Assuming that the wave action is perpendicular to the caisson array axis (i.e., y-direction), vibration responses along with the y-direction are dominant (Lee *et al*. 2011, 2012, Yoon *et al*. 2012). This study is limited to take into account only for the horizontal displacement (e.g., sway motion) which is measurable in the caisson system by the use of uni-directional sensor orientation. As shown in Fig. 1(b), caissons are treated as rigid bodies on elastic half-space foundations which can be described via the horizontal springs and dashpots (Huynh *et al*. 2013). Horizontal spring and dashpots with respect to three caissons are defined, respectively. To represent the condition of the interlocking mechanism, springs and dashpots are also simulated between adjacent caisson units.

By equating to the equilibrium conditions of the free-body diagrams, as shown in Fig. 1(b), the horizontal displacement can be formulated in matrix form as

$$[\mathrm{M}]\{\ddot{u}\} + [\mathrm{C}]\{\dot{u}\} + [\mathrm{K}]\{u\} = \{\mathrm{F}\} \tag{1}$$

in which [M], [K] and [C] represent the mass matrix, stiffness matrix, and damping matrix, respectively; and $\{F\}$ is the vector of external force. As shown in Fig. 1(b), structural properties of the caisson system are defined as follows: m_j is the total horizontal mass of the j^{th} caisson; k_{Fj} and c_{Fj}, respectively, represent the horizontal spring and damping coefficients of the j^{th} caisson's foundation (j=1-3); k_{Sk} and c_{Sk}, respectively, represent the horizontal spring and dashpot of the n^{th} shear-key connection (n=1-4); the symbols $\ddot{u}_j, \dot{u}_j$ and u_j are, respectively, the horizontal acceleration, velocity and displacement of the j^{th} caisson; and $P_j(t)$ is the external force placed at the center of gravity of the j^{th} caisson.

When the caisson is oscillated by an impulse load, its boundary media (i.e., soil and water) are also forced to move with the structure. Therefore, the total horizontal mass of the j^{th} caisson (m_j) includes not only the mass of the caisson (m_j^{cai}) but also the contribution from horizontal hydrodynamic mass (m_j^{hyd}) and horizontal geodynamic mass (m_j^{geo}), as follows

$$m_j = m_j^{cai} + m_j^{hyd} + m_j^{geo} \tag{2}$$

To calculate the horizontal hydrodynamic mass (m_j^{hyd}), the equation presented by Oumeraci and Kortenhaus (1994) is used

$$m_j^{hyd} = 0.543\rho_w L_j {H_{w_j}}^2 \tag{3}$$

in which the quantities L_j and H_{w_j} are the j^{th} caisson's length and the water level, respectively, as shown in Fig. 1(a); and the quantity ρ_w is the mass density of sea water. According to Richart *et al*. (1970), the horizontal geodynamic mass can be computed as

$$m_j^{geo} = 0.76\rho_s\left(\frac{B_jL_j}{\pi}\right)^{3/2} / (2-\nu) \tag{4}$$

where ρ_s and ν are, respectively, the mass density and Poisson's ratio of the foundation soil; and B_j is the j^{th} caisson's width, as sketched in Fig. 1(a).

As adopted by Goda (1994) and Vink (1997), the horizontal spring constant (k_{Fj}) of the elastic foundation is modeled as the function of the horizontal modulus of subgrade reaction *(b)*, as follows

$$k_{Fj} = bL_jB_j \tag{5}$$

in which the modulus of subgrade reaction *(b)* is available for various soil types as reported by Bowles (1996). Note that the modulus has the unit of pressure per length.

Next, the stiffness of the middle shear keys is modeled as $k_{S2} = k_{S3}$ by assuming that caisson segments are designed with the uniform linking capacity. However, it is assumed that the stiffness of the last shear keys (i.e., k_{S1} and k_{S4}) is smaller than that of the middle shear keys (i.e., k_{S2} and k_{S3}).

$$k_{S1} = k_{S4} = pk_{F1} \quad \text{and} \quad k_{S2} = k_{S3} = qk_{F2} \tag{6}$$

in which p and q are stiffness ratios with respect to k_F. Note that the theoretical basis for the shear-key's stiffness is relatively small as compared to the foundation's stiffness, since it depends on the linking capacity between contacted units in the real caisson breakwater (Oumeraci *et al*. 2001).

The Rayleigh damping, which is often used in the dynamic mathematical model, is used to simulate the energy dissipation in the caisson system. The Rayleigh damping is assumed to be proportional to the mass and stiffness matrices (Wilson 2004)

$$[\mathrm{C}] = \alpha[\mathrm{M}] + \beta[\mathrm{K}] \tag{7}$$

in which α is the mass-proportional damping coefficient; and β is the stiffness-proportional damping coefficient. Due to the orthogonality condition of the mass and stiffness matrices, this equation can be rewritten as

$$\xi_i = \frac{1}{2\omega_i}\alpha + \frac{\omega_i}{2} \tag{8}$$

in which ξ_i is the critical-damping ratio for i^{th} mode; and ω_i is the i^{th} natural frequency. If the damping ratios corresponding to two specific frequencies (e.g., ω_e and ω_f) are known, the two Rayleigh damping factors (i.e., α and β) can be evaluated from the following equation

$$\begin{bmatrix}\xi_e\\ \xi_f\end{bmatrix} = \frac{1}{2}\begin{bmatrix}\frac{1}{\omega_e} & \omega_e\\ \frac{1}{\omega_f} & \omega_f\end{bmatrix}\begin{bmatrix}\alpha\\ \beta\end{bmatrix} \tag{9}$$

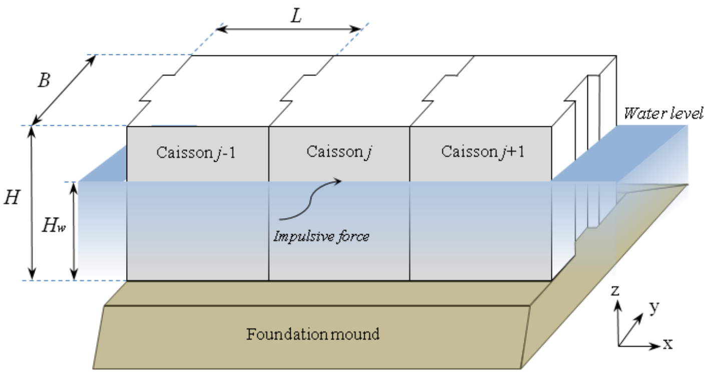

(a) Caisson system of three units

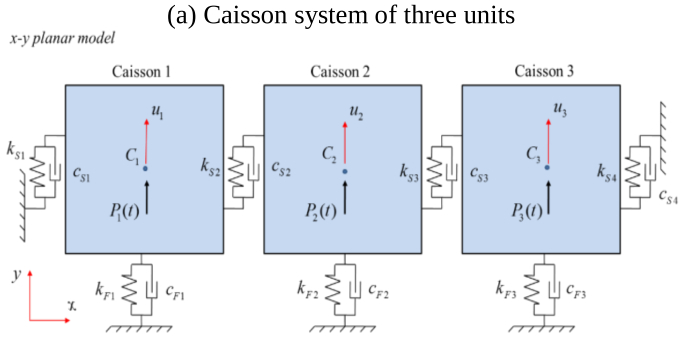

(b) Simplified model of caisson system

Fig. 1 A caisson system of three units and its simplified model (Huynh *et al*. 2013)

When damping ratios for both frequencies are set to an equal value, $\xi_e = \xi_f = \xi$, the Rayleigh damping factors are calculated as (Wilson 2004)

$$\beta = \frac{2\xi}{\omega_e + \omega_f} \quad \text{and} \quad \alpha = \omega_e \omega_f \beta \tag{10}$$

3. Vibration-based structural identification algorithm

For the performance assessment of the gravity-type caisson system, our interest is to analyze exactly how the structure will respond under given excitation conditions and, especially, with what amplitudes. This will depend on the structure's inherent properties (such as stiffness, mass and damping) and also on the nature and magnitude of the applied excitation (Ewins 2000). For most of real harbor caisson structures, however, it is almost impossible to impose the excitation enough for meaningful responses. An alternative way is to choose a standard excitation and to describe the responses as a set of frequency response functions (FRFs) based on a unit-amplitude sinusoidal force applied to the structure. There exists the interdependence between the structural parameters and the modal responses (e.g., FRFs, natural frequency and damping); therefore, the structural parameters (e.g., stiffness, mass and damping) can be identified from the inverse analysis of the measured response properties. Once accurately identified, the structural model may represent the estimation of field responses corresponding to any design forces on the real structure. Based on this concept, in this study, a structural identification algorithm is designed for the gravity-type caisson structure system.

3.1 Vibration response analysis

As stated in Eq. (1), a structural model is represented by structural dynamic characteristics such as stiffness, mass, and damping properties. Its acceleration responses depend on the structural characteristics and it can be defined as

$$\ddot{u}_t = [\mathrm{M}]^{-1}\left(\{F\} - \dot{u}_t[\mathrm{C}] - u_t[\mathrm{K}]\right) \tag{11}$$

where u_t, $\dot{u}_t$ and $\ddot{u}_t$ represent the displacement, velocity, and acceleration vectors, respectively; [M], [K] and [C] represent the mass matrix, stiffness matrix, and damping matrix, respectively; and $\{F\}$ is the vector of external force. The acceleration response provides an understanding of the dynamic characteristics that represent the structural behaviors. In this study, piezoelectric accelerometers are utilized to measure the acceleration responses. The piezoelectric material in the sensor acts as a spring and connects the base of the accelerometer to a seismic mass. When an input is introduced to the base, a force is created on the piezoelectric element that is proportional to the applied acceleration and the size of the seismic mass.

For the forced response of a damped structural system, the general receptance FRF can be simplified in a complex form as follows (Ewins 2000)

$$[\Omega(\omega)] = \left[\mathrm{K} + i\omega\mathrm{C} - \omega^2\mathrm{M}\right]^{-1} \tag{12}$$

in which the receptance $\Omega(\omega)$ is defined as force to displacement response ratio in frequency domain, so that Eq. (11) can be interpreted as Eq. (12). Due to the orthogonal condition of mass and stiffness matrices, the damped system can be evaluated for the i^{th} vibration mode, as follows

$$\bar{\omega}_i^2 = \omega_i\sqrt{1-\xi_i^2} \tag{13a}$$

$$\xi_i = \beta\omega_i/2 + \alpha\omega_i/2 \tag{14b}$$

where ξ_i is the i^{th} critical-damping ratio; ω_i is the i^{th} undamped natural frequency; and $\bar{\omega}_i$ is the i^{th} damped natural frequency. If the damping ratios (e.g., ξ_e and ξ_f) corresponding to two specific undamped natural frequencies (e.g., ω_e and ω_f) are known, the two Rayleigh damping factors (i.e., β and α) can be evaluated from Eq. (10).

As shown in Fig. 2(a), the simplest peak-picking method is adopted for analyzing measured FRF data to obtain the simplified model of the target caisson structure described in Fig. 1. The resonance peak is detected on the FRF plot and the frequency of the maximum response is taken as the i^{th} natural frequency (ω_i). Also, the i^{th} modal amplitude can be taken at the maximum response. Next, the local maximum value of measured FRF is noted as $|H|$. The frequency bandwidth of the function for a response level of $|H|/\sqrt{2}$ is determined as the two half-power points, ω_a and

ω_b. Then the damping of the i^{th} mode can be experimentally estimated from the following formula (Ewins 2000)

$$\xi_i = \left(\omega_a^2 - \omega_b^2\right) \Big/ 2\omega_i^2 \tag{15}$$

Assume there are two different systems, i.e., experimental state (noted as 'E') and analytical model (noted as 'A'), as shown in Fig. 2(b). Then their systematic differences in structural parameters can be quantified by estimating changes in vibration features like natural frequencies and FRFs. In this study, the change in eigenvalues is used to represent the change in stiffness parameter. Also, the change in FRFs is used for the change in damping parameter.

3.2 Structural identification algorithm

Kim and Stubbs (1995) proposed a system identification method to identify a realistic theoretical model of a structure by using vibration modal parameters. Based on their method, in this study, structural identification is mainly performed in two steps: first, an initial structural model is designed based on geometrical and material properties and boundary conditions; and next, structural parameters (e.g., stiffness and damping) are identified by fine-tuning modal parameters.

Suppose p_j^* is an unknown structural parameter (i.e., mass, stiffness, or damping parameters) of the j^{th} member of a structure for which modal parameters (i.e., natural frequencies and damping coefficients) are known for *M* vibration modes. Also, suppose p_j is a corresponding known structural parameter of the j^{th} member of an analytical model for which the corresponding set of modal parameters are known for the same *M* vibration modes.

Relative to the target structure, the structural parameter of the j^{th} member of the analytical model is defined as follows

$$p_j^* = p_j + \delta\ \ p \tag{16}$$

in which δp_j is the variation of the structural parameter of the j^{th} member which results in changes of modal parameters. The sensitivity S_{ij} of the i^{th} damped eigenvalue $\bar{\omega}_i^2$ with respect to the j^{th} structural parameter p_j is defined as follows

$$S_{ij} = \frac{\delta\bar{\omega}_i^2}{\delta p_j}\frac{p_j}{\bar{\omega}_i^2} \tag{17}$$

in which the damped eigenvalue is defined as $\bar{\omega}_i^2 = \omega_i^2(1-\xi_i^2)$. Since the sensitivity S_{ij} is related to the combination of the undamped natural frequency and damping coefficient, a simplified approach is needed to analyze the sensitivity with respect to each parameter.

<u>Stiffness Parameter Identification</u>

By fixing the damping coefficient as constant from Eq. (17), the stiffness sensitivity S_{ij}^S of the i^{th} undamped eigenvalue ω_i^2 with respect to the j^{th} stiffness parameter k_j is defined as

$$S_{ij}^S = \frac{\delta\omega_i^2}{\delta k_j}\frac{k_j}{\omega_i^2} \tag{18}$$

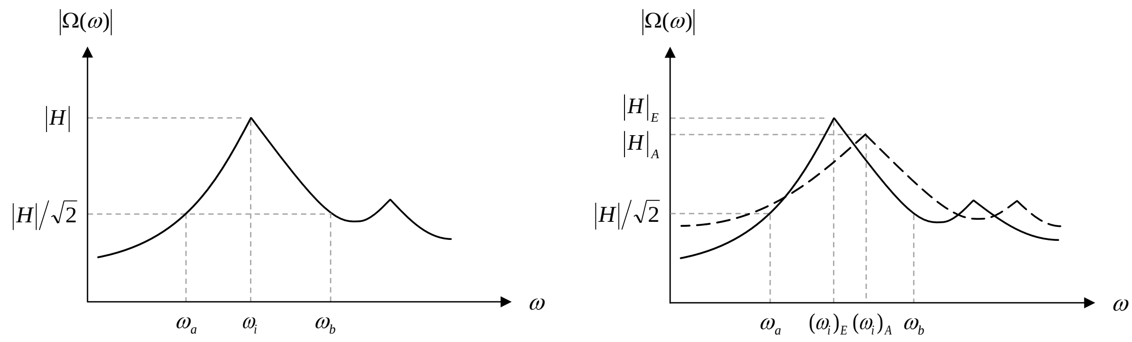

(a) FRF plot (b) Experiment versus analytical model

Fig. 2 FRF analysis by peak picking method

where δk_j is the first order perturbation of k_j which produces the variation in eigenvalue $\delta\omega_i^2$.

The fractional change in stiffness parameters of NE members may be obtained using the following equation (Kim and Stubbs 1995)

$$\left\{\delta k_j / k_j\right\} = \left[S^S\right]^{-1}\left\{Z^S\right\} \tag{19}$$

where $\left\{\delta k_j / k_j\right\}$ is a $NE \times 1$ matrix containing the fractional changes in stiffness parameters between the analytical model and the target structure; $\left\{Z^S\right\}$ is a $M \times 1$ matrix containing the fractional changes in eigenvalues between two systems; and $\left[S^S\right]$ is a $M \times NE$ dimensionless stiffness sensitivity matrix. The convergence between the measured and analytical eigenvalues is estimated by the fractional changes in eigenvalues between the experimental state and the analytical model, as follows

$$\left|Z_i^S\right| = \left|\frac{\omega_{i,m}^2 - \omega_{i,a}^2}{\omega_{i,a}^2}\right| \tag{20}$$

in which $\omega_{i,m}^2$ and $\omega_{i,a}^2$ are the i^{th} eigenvalues of the measured target structure and the analytical model, respectively. The completeness of the model update is identified as the convergence approaches to a tolerance value.

<u>Damping Parameter Identification</u>

By fixing the undamped eigenvalue as constant from Eq. (17), the damping sensitivity S_{ij}^D of the i^{th} modal damping coefficient ξ_i^2 with respect to the j^{th} structural damping parameter c_j is defined as

$$S_{ij}^{D} \approx \frac{\delta \xi_i^2}{\delta c_j} \frac{c_j}{\left(\xi_i^2 - 1\right)} \tag{21}$$

where δc_j is the first variation of c_j which produces the variation in damping coefficient $\delta \xi_i$.

The fractional change in structural damping parameters of NE members may be obtained as follows

$$\left\{\delta c_j / c_j\right\} = \left[S^{D}\right]^{-1} \left\{Z^{D}\right\} \tag{22}$$

where $\left\{\delta c_j / c_j\right\}$ is a $NE \times 1$ matrix containing the fractional changes in damping parameters between the analytical model and the target structure; $\left\{Z^{D}\right\}$ is a $M \times 1$ matrix containing the fractional changes in damping coefficients between two systems; and $\left[S^{D}\right]$ is a $M \times NE$ dimensionless damping sensitivity matrix. The fractional change in damping coefficients between the experimental state and the analytical model is estimated as follows

$$\left|Z_i^{D}\right| = \left|\frac{\xi_{i,m}^2 - \xi_{i,a}^2}{\xi_{i,a}^2 - 1}\right| \tag{23}$$

in which $\xi_{i,m}^2$ and $\xi_{i,a}^2$ represent the i^{th} damping eigenvalues of the measured target structure and the analytical model, respectively.

The reliability of Eq. (23) depends rather upon the quality of experimental damping values. Moreover, the accuracy of damping coefficients extracted from real structures is not guaranteed for most of civil engineering structures. So there should be an alternative way to identify the convergence of damping parameters for the gravity-type caisson system, in which experimental damping estimation would not be accurate. Our choice is power spectral density (PSD) which efficiently represents all of modal characteristics and also minimizes the noise effects. The PSD is utilized to examine the change in damping property as much as the change in modal amplitude. The PSD $S(f)$ can be calculated by Welch's procedure

$$S(f) = \frac{1}{n_d T} \sum_{i=1}^{n_d} \left|Y_i(f,T)\right|^2 \tag{24}$$

in which $Y_i(f,T)$ is FFT result of the acceleration signal. To estimate the change in the frequency response due to the change in structural properties, the root mean square deviation (RMSD) of PSDs is calculated as follows

$$RMSD(S_A, S_E) = \sqrt{\frac{\sum\left[S_E(f) - S_A(f)\right]^2}{\sum\left[S_A(f)\right]^2}} \tag{25}$$

where $S_A(f)$ and $S_E(f)$ are the PSDs of the analytical model and the experimental state, respectively. The convergence between the measured and analytical damping properties is identified as the RMSD close to zero.

4. Experimental vibration analysis of lab-scale caisson structure

4.1 Description of test Set-up

As shown in Fig. 3, a lab-scale caisson model is selected as the target structure. Four main subsystems include caisson body, cap concrete, two adjacent blocks, and foundation mound. The caisson's height and width are square as 34 cm and 34 cm; it also includes the empty inner space with vertical wall of 5 cm thickness. The cap concrete's height is 10 cm at the maximum. Bottom dimension of the cap concrete is the same as that of the caisson. Due to the limited width of the 2-D wave flume, two adjacent caissons were replaced by adopting concrete blocks which have 6 cm thickness to make the main caisson body fitted into the side wall of the wave flume. Each caisson body has shear keys for interlocking between adjacent caisson bodies.

Vibration responses were measured by a data acquisition system consisting of accelerometers (PCB 393B04 model with $\pm$ 5g of measureable range and 1 V/g of sensitivity), a signal conditioner, a DAQ card, and a laptop. As shown in Fig. 3, the accelerometers were installed at the top of the cap concrete to measure the vibration response of the caisson. For the design of sensor locations in the lab caisson, the limited accessibility of coastal and harbor caisson systems was considered since the partially-submerged on-site condition imposed restrictions on the possibility of extracting modal parameters from the entire caisson geometry.

In this study, rigid body motions were selected as the target behaviors of the test caisson. Note that the rigid body motion is defined when deformation of caisson is much smaller than deformation of foundation mound. It has been reported that the rigid body motion is sensitive to the variation of foundation integrity (Lee *et al*. 2012, Huynh *et al*. 2013). According to the previous studies by Ming *et al*. (1988) and Lee *et al*. (2012), the first a few modes corresponding to the rigid body motions could be extracted from the field tests and even from lab tests for the caisson structure.

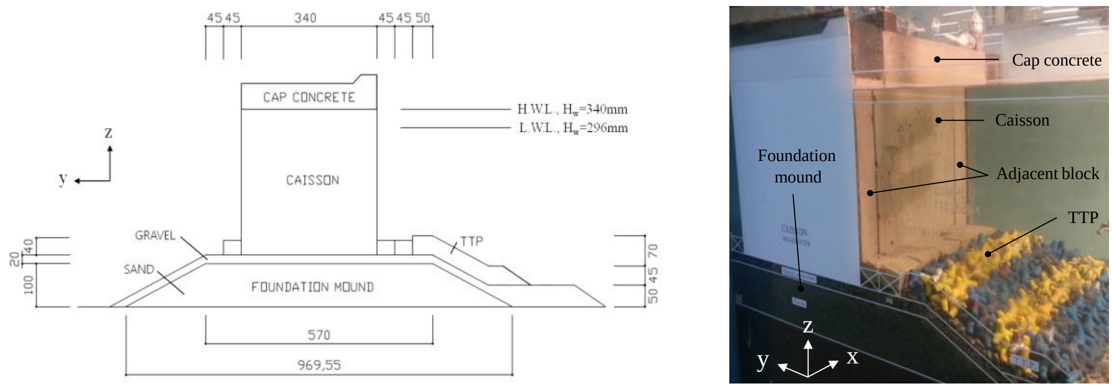

Fig. 3 Test setup in the 2-D wave flume

To extract the vibration characteristics corresponding to the rigid body motions of the test caisson, sensors were installed at four points along with y-and z-axes. Acceleration signals were acquired for 20 seconds at 500 Hz of sampling rates. Impact excitations that simulate ship collisions were implemented by using a rubber hammer applied on the front wall of the caisson. The impact was manually applied by a test implementer. Further details on the lab tests are described in Lee *et al*. (2013).

4.2 Test scenarios and vibration responses

Mainly two different conditions were considered for estimating their effects on structural properties and vibration characteristics of the lab-scale caisson system. The first condition is water-level variation from high water level (HWL) to low water level (LWL) and the second one is foundation damage like the cavity in found mound. As the test scenarios, three cases were select as: (1) an undamaged reference structure with HWL, (2) an undamaged structure with water-level change into LWL, and 3) a foundation-damaged structure with HWL (i.e., no water-level change).

To simulate the water-level variation, two water-levels were designed in 2-D wave flume. As indicated in Fig. 3, the HWL and the LWL were selected based on on-site tidal conditions near Busan, Korea. They vary about 1.2 m during high and low tides and it was scaled down as 44mm as the depth variation. The caisson was kept undamaged during the tests.

Next, damage was inflicted into the foundation mound of the caisson system and changes in modal parameters were estimated. The water level was fixed as the HWL during the test. The occurrence of the foundation damage is typically caused by dislocation of wave-dissipating blocks and subsequent scouring induced by repeated extreme wave actions. In this study, the damage was simulated by removing some parts of armor blocks and TTP blocks from the foundation mound, which caused 18.7% loss out of the bottom area of the caisson.

The test caisson was excited by hammer impact and acceleration responses were measured by the vibration measurement system. Fig. 5 shows the y-directional and z-directional vibration responses measured at the acquisition point 1. Note that the y-direction corresponds to wave incident direction. The maximum y-directional acceleration was about 0.25 g with short impulse duration; meanwhile, the maximum z-directional acceleration was less than 0.1 g.

The peak picking method was implemented to extract frequency responses and modal parameters for the three test cases. For the case of ‘the undamaged reference structure with HWL’, the power spectral density was extracted from the acceleration signal measured from the sensor 1-y (see Fig. 4). For the analysis of the reference caisson with HWL, the first two modes were extracted by using the stochastic subspace identification (SSI) method and the frequency-domain decomposition (FDD) method (Yi and Yun 2004, Lee *et al*. 2013). The extracted natural frequencies are sketched as shown in Fig. 6. The first two natural frequencies were observed at about 17 Hz and 42 Hz in both results of the FDD method and the SSI method. The first two damping coefficients were about 6.9% and 2.7%, respectively.

For all three test cases, natural frequencies and damping coefficients were extracted as listed in Table 1. From the results, it is observed that the natural frequencies increased as the water level decreased (i.e., as HWL turns to LWL) but they decreased as the foundation damage occurred. It is also observed that damping ratios were inconsistent in mode 1 and mode 2. In mode 1, damping ratios were decreased by water-level decrease but increased by damage occurrence. In mode 2, however, there was almost no change. Also, the change in damping ratio due to the ground damage seemed to be overestimated.

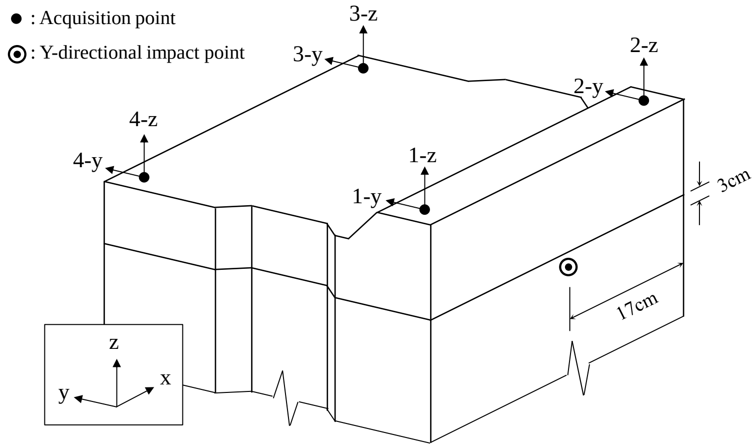

Fig. 4 Orientation of sensors and excitation point (Lee *et al*. 2013)

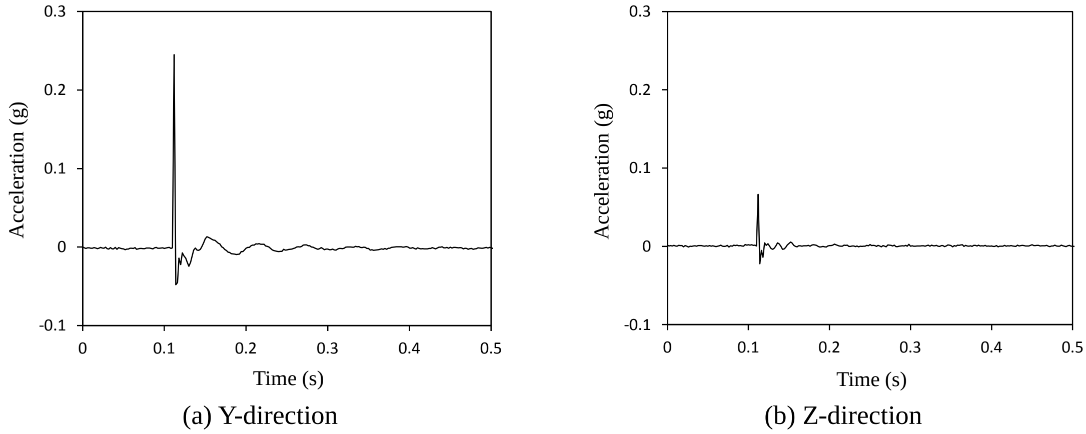

Fig. 5 Acceleration responses at acquisition point 1 excited by hammer impact

Table 1 Experimental modal parameters of test caisson system for three test cases

Test scenario	Natural frequency (Hz)		Damping ratio (%)			
			Peak-Picking		SSI	
	Mode 1	Mode 2	Mode 1	Mode 2	Mode 1	Mode 2
Undamaged HWL	17.33	41.99	6.89	2.74	7.14	4.00
Undamaged LWL	19.78	44.68	5.26	2.64	6.20	N/A
Damaged HWL	15.39	42.24	12.08	2.89	6.89	3.50

To check the reliability of the extracted damping ratios from the peak-picking method, the SSI method was also utilized to extract damping ratios. As listed in Table 1, damping ratios extracted by the SSI method were also inconsistent as compared to those by the peak-picking method. Due to the inconsistent quality of experimental damping values, the alternative way utilizing PSDs and RMSD (as described in Eqs. (24) and (25)) should be utilized to identify the convergence of damping parameters of the caisson structure system.

5. Vibration-based structural identification of lab-scale caisson structure

5.1 Structural identification for reference structure

Initial Structural Model

The structural model of 'the undamaged reference structure with HWL' was initially established by using geometry of the test structure and the experimental modal parameters. The total horizontal masses were computed with 0.34 m of the water height as $m_1 = m_3 = 22.95$ kg and $m_2 = 138.06$ kg by using Eqs. (2)-(4). The diagonal components of the M matrix consisted of the mass of concrete, the mass of water filled, the added mass of sea water, and the added mass of foundation soil.

The modulus of sub-grade reaction of the foundation mound, *b*, was selected as 9.6 MN/m for medium dense sand (Bowles 1996). By using Eq. (5), the spring constants of the foundation mound were calculated as $k_{F1} = k_{F3} = 1.824\text{x}10^5$ N/m and $k_{F2} = 1.110\text{x}10^6$ N/m. By assuming stiffness ratios as $p = 1$, and $q = 0.5$ for the initial model, the stiffness of the middle and last shear-keys were obtained as $k_{S1} = k_{S4} = 1.824\text{x}10^5$ N/m and $k_{S2} = k_{S3} = 5.549\text{x}10^5$ N/m, respectively. As the initial damping parameter, the two Rayleigh damping coefficients were computed from Eq. (13) by using the first two natural frequencies ($\omega_1 = 17.33$ Hz, $\omega_2 = 41.99$ Hz) and the damping ratio ($\xi_1 = 6.89$ %, $\xi_2 = 2.74$ %). In Table 2, the calculated K and C matrices of the initial structural model are summarized in forms of relative values.

To solve the equation of motion (see Eq. (1)), the Runge-Kutta scheme was utilized as supported in Matlab 7.9.0.529. Time interval was set as 0.001 second for the calculation of vibration responses. As shown in Fig. 7, the acceleration and PSD responses of the initial structural model were compared with those of the experimental state of 'the undamaged caisson with HWL'. It is observed that the two acceleration responses show differences in dissipation and oscillating period. It is also observed that the two PSD curves are quite different in the peaks and the dissipation slopes. Note that the initial impact force was assumed as 1N in the numerical simulation. It was assumed that relationship between acceleration response and impact force is linear. Then, impact force of the simulation was determined to the value which gives similar response to experimental response in the maximum acceleration.

Model Update: Stiffness Parameter

The stiffness parameters were updated by using the trial-and-error method to improve the convergence of the structural model to the experimental state. The stiffness ratios, *p* and *q*, of Eq. (6) controlled to adjust the peak frequencies of power spectral density. As the result of the stiffness parameter update, the stiffness ratios were selected as p=1.5 and q=0.8, so that the stiffness of the shear-keys was updated as $k_{S1} = k_{S4} = 2.736\text{x}10^5$ N/m and $k_{S2} = k_{S3} = 8.880\text{x}10^5$ N/m, respectively. The calculated K matrix and C matrix with the updated stiffness parameters are summarized in Table 2.

As shown in Fig. 8, the acceleration and PSD responses of the stiffness-updated model were compared with those of the experimental state. It is observed that the two acceleration responses show very close oscillating period but difference in dissipation. It is also observed that the two PSD curves are similar in the natural frequencies but different in the dissipation slopes. Note that the stiffness parameters were updated using the trial-and-error method. In general, the manual tuning might not be objective; however, the process might be one of the choices due to the complexity of the structural and response parameters.

Model Update: Damping Parameter

The damping parameters were updated by using the trial-and-error method to improve the convergence of the structural model's dissipation of vibration responses to that of the experimental state. The damping parameters, ξ_1 and ξ_2, were used as updating parameters to adjust the peak dissipation of power spectral density. As the result of the damping parameter update, the damping ratios are selected as ξ_1=15.17%, ξ_2=10.98%, respectively. The calculated K and C matrices with the updated damping parameters are summarized in Table 2.

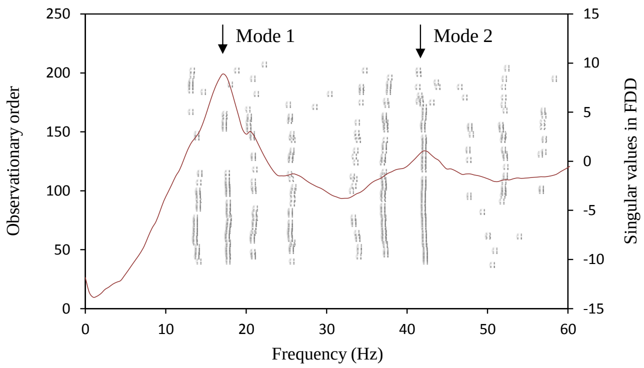

Fig. 6 SSI method's stabilization charts and FDD method's singular values for the undamaged reference caisson with HWL

Table 2 Estimated structural parameters for 'the undamaged reference caisson with HWL'

	Stiffness ratio	K matrix	C matrix
Initial	$k_{S1} = k_{S4} = k_{F1}$ $k_{S2} = k_{S3} = 0.5k_{F2}$	$\begin{bmatrix} 0.92 & -0.55 & 0 \\ -0.55 & 2.22 & -0.55 \\ 0 & -0.55 & 0.92 \end{bmatrix} \times 10^6$	$\begin{bmatrix} 0.34 & 0.01 & 0 \\ 0.01 & 2.07 & 0.01 \\ 0 & 0.01 & 0.34 \end{bmatrix} \times 10^3$
Stiffness update	$k_{S1} = k_{S4} = 1.5k_{F1}$ $k_{S2} = k_{S3} = 0.8k_{F2}$	$\begin{bmatrix} 1.34 & -0.89 & 0 \\ -0.89 & 2.89 & -0.89 \\ 0 & -0.89 & 1.34 \end{bmatrix} \times 10^6$	$\begin{bmatrix} 0.33 & 0.01 & 0 \\ 0.01 & 2.06 & 0.01 \\ 0 & 0.01 & 0.33 \end{bmatrix} \times 10^3$
Damping update	$k_{S1} = k_{S4} = 1.5k_{F1}$ $k_{S2} = k_{S3} = 0.8k_{F2}$	$\begin{bmatrix} 1.34 & -0.89 & 0 \\ -0.89 & 2.89 & -0.89 \\ 0 & -0.89 & 1.34 \end{bmatrix} \times 10^6$	$\begin{bmatrix} 1.22 & -0.38 & 0 \\ -0.38 & 5.10 & -0.38 \\ 0 & -0.38 & 1.22 \end{bmatrix} \times 10^3$

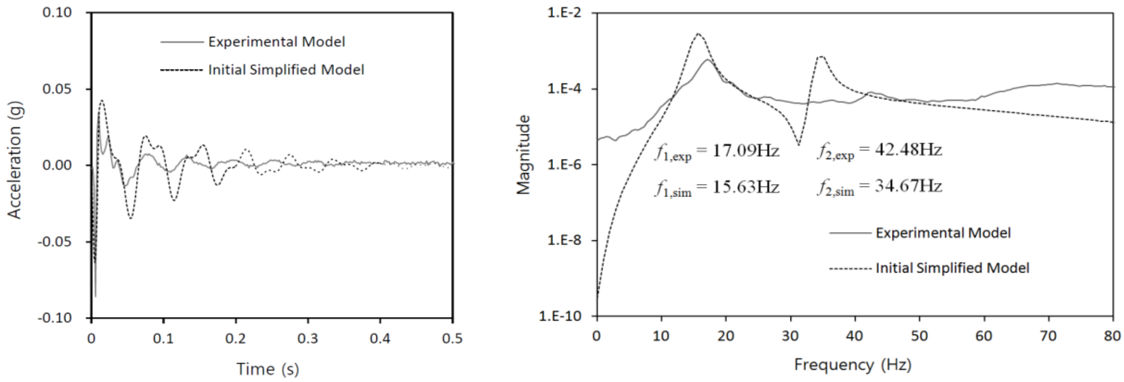

(a) Acceleration response (b) Power spectral density

Fig. 7 Vibration responses of initial model for ‘the undamaged caisson with HWL’

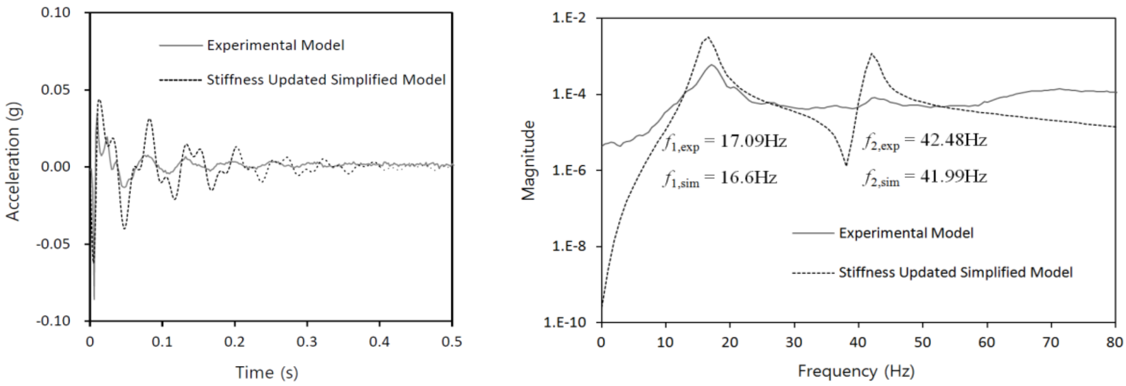

(a) Acceleration response (b) Power spectral density

Fig. 8 Vibration responses of stiffness-updated model for ‘the undamaged caisson with HWL’

As shown in Fig. 9, the acceleration and PSD responses of the damping-updated model were compared with those of the experimental state. It is observed that the two acceleration signals are well-matched. Two responses show very close oscillating period and also in dissipation. It is also observed that the two PSD curves are well-matched both the peak frequencies and the dissipation slopes. Note that the primary motivation of updating the damping parameter is to identify the energy dissipation capacity, so that the update damping parameters represents the energy dissipation capacity.

The accuracy of the structural models was assessed by the eigenvalue index (i.e., the fraction change in eigenvalues defined as Eq. (20)) and the RMSD index (i.e., the root-mean-square-deviation of power spectral densities defined by Eq. (25)). Note that two frequency bands 13.67 - 22.46 Hz and 40.04 - 49.81 Hz were utilized for the RMSD estimation. Table 3 shows the estimated similarities of structural parameters (i.e., stiffness and damping) of the three structural models (i.e., initial, stiffness-updated, and damping-updated models) as compared to the experimental state of ‘the undamaged caisson with HWL’. It is observed that the eigenvalue indices of the two modes converge as stiffness updated. It is also observed that the RMSD indices converge as damping updated. Note that the convergence results verify the successful identification of the structural model corresponding to ‘the undamaged caisson with HWL’.

5.2 Structural identification for water-level change

The undamaged structure with LWL was analyzed for structural identification for water-level change. It is noted that the water-level was varied from HWL to LWL to estimate its effect on vibration characteristics as much as structural properties. The initial model was based on the damping-updated model (see Table 2) for the undamaged caisson with HWL. By assuming that the water level is known, the water height was adjusted as 0.296 m in the initial modeling. Therefore, the total horizontal masses of considering the water level were estimated as: $m_1 = m_3 = 21.25$ kg and $m_2 = 127.72$ kg. As outlined in Table 4, the stiffness ratios of the initial model were the same as the final damping-updated model for the undamaged caisson with HWL. Next, the first two natural frequencies ($\omega_1 = 19.78$ Hz and $\omega_2 = 44.68$ Hz) and the corresponding damping ratios ($\xi_1 = 5.26$ % and $\xi_2 = 2.64$ %) were utilized for the calculation of the two Rayleigh damping coefficients of Eq. (13).

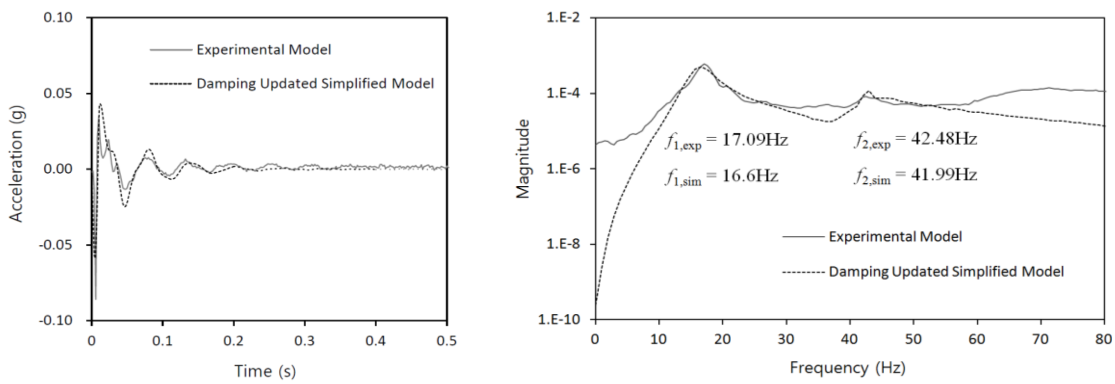

(a) Acceleration response (b) Power spectral density

Fig. 9 Vibration responses of damping-updated model for ‘the undamaged caisson with HWL’

Table 3 Convergence of structural models to ‘the undamaged reference caisson with HWL’

	Eigenvalue index		RMSD index	
	Mode 1	Mode 2	Mode 1	Mode 2
Initial	0.1955	0.5013	0.1373	0.0256
Stiffness update	0.0599	0.0235	0.1288	0.1330
Damping update	0.0599	0.0235	0.0247	0.0231

Table 4 Estimated structural parameters for ‘the undamaged caisson with LWL’

	Stiffness ratio	K matrix	C matrix
Initial	$k_{S1} = k_{S4} = 1.5k_{F1}$ $k_{S2} = k_{S3} = 0.8k_{F2}$	$\begin{bmatrix} 1.34 & -0.89 & 0 \\ -0.89 & 2.89 & -0.89 \\ 0 & -0.89 & 1.34 \end{bmatrix} \times 10^6$	$\begin{bmatrix} 1.27 & -0.59 & 0 \\ -0.59 & 3.54 & 0.59 \\ 0 & -0.59 & 1.27 \end{bmatrix} \times 10^3$
Stiffness updated	$k_{S1} = k_{S4} = 5.76k_{F1}$ $k_{S2} = k_{S3} = 0.43k_{F2}$	$\begin{bmatrix} 1.49 & -0.40 & 0 \\ -0.40 & 2.13 & -0.40 \\ 0 & -0.40 & 1.49 \end{bmatrix} \times 10^6$	$\begin{bmatrix} 0.30 & -0.02 & 0 \\ -0.02 & 1.49 & -0.02 \\ 0 & -0.02 & 0.30 \end{bmatrix} \times 10^3$
Damping updated	$k_{S1} = k_{S4} = 5.76k_{F1}$ $k_{S2} = k_{S3} = 0.43k_{F2}$	$\begin{bmatrix} 1.49 & -0.40 & 0 \\ -0.40 & 2.13 & -0.40 \\ 0 & -0.40 & 1.49 \end{bmatrix} \times 10^6$	$\begin{bmatrix} 1.19 & -0.20 & 0 \\ -0.20 & 3.81 & -0.20 \\ 0 & -0.20 & 1.19 \end{bmatrix} \times 10^3$

Table 4 outlines the calculated K and C matrices of the structural models in forms of relative values. For the stiffness and damping updates, the procedures were performed the same as described previously. Fig. 10 shows vibration responses of the initial model for the test case of “the undamaged caisson with LWL”. Fig. 11 shows vibration responses of the stiffness-updated model for the test case. Fig. 12 shows vibration responses of the damping-updated model for the test case. From the figures, it is observed that the two acceleration signals the two PSD curves become matched each other in the oscillating period, the peak frequencies and the dissipation slopes.

Table 5 outlines the estimated similarities of structural parameters of the updated models as compared to the experimental state of ‘the undamaged caisson with LWL’. It is observed that the eigenvalue indices converge as stiffness updated and the RMSD indices converge as damping updated. Note that the convergence results verify the successful identification of the structural model corresponding to the water level change in the caisson system.

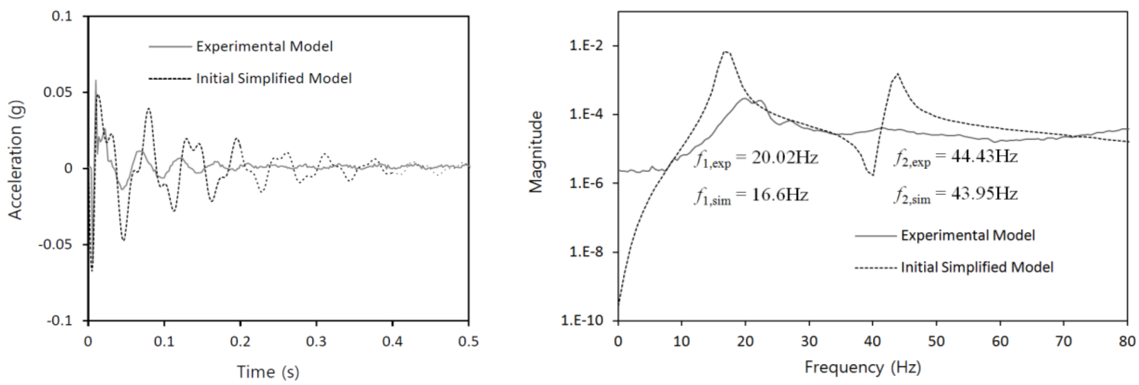

(a) Acceleration response (b) Power spectral density

Fig. 10 Vibration responses of initial model for ‘the undamaged caisson with LWL’

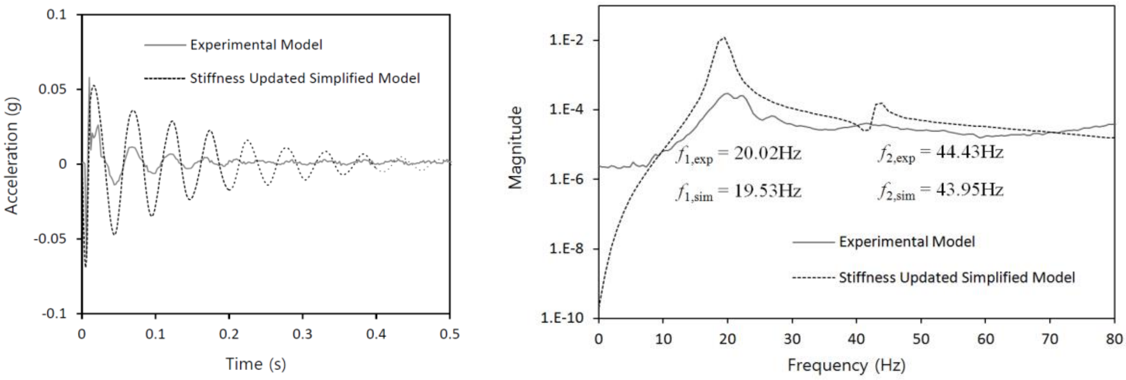

(a) Acceleration response (b) Power spectral density

Fig. 11 Vibration responses of stiffness-updated model for 'the undamaged caisson with LWL'

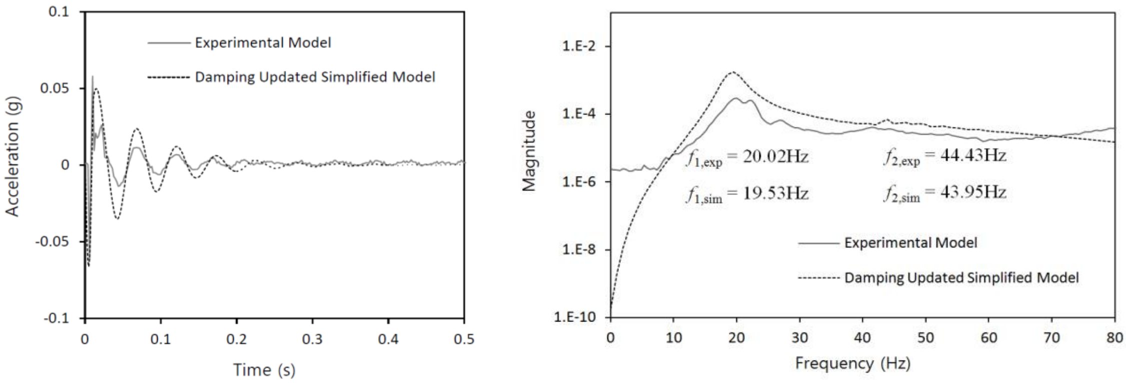

(a) Acceleration response (b) Power spectral density

Fig. 12 Vibration responses of damping-updated model for 'the undamaged caisson with LWL'

Table 5 Convergence of structural models to 'the undamaged caisson with LWL'

	Eigenvalue index		RMSD index	
	Mode 1	Mode 2	Mode 1	Mode 2
Initial	0.4545	0.0220	0.2863	0.2137
Stiffness update	0.0508	0.0220	0.2667	0.0815
Damping update	0.0508	0.0220	0.1573	0.0521

As the water levels changed from HWL to LWL (see Fig. 3), i.e., the water height decreased by 13%, natural frequencies were increased and damping coefficients were slightly decreased as outlined in Table 1. From the comparison of the identified structural model for the reference structure (Table 2) to the corresponding one for the water-level variation into LWL (Table 4), it is observed that system stiffness (indicated by K matrix) slightly increased and system damping (indicated by C matrix) slightly decreased due to the water height decrement.

5.3 Structural identification for foundation damage

The damaged structure with HWL was analyzed for structural identification for foundation damage. It is noted that the foundation damage was inflicted into the test structure to estimate its effect on vibration characteristics as much as structural properties. The initial model was based on the damping-updated model (see Table 2) for the undamaged caisson with HWL. It was assumed that the water level is known. The total horizontal masses, therefore, were computed for 0.34 m of water level for the diagonal components as $m_1 = m_3 = 22.95$ kg and $m_2 = 138.06$ kg). As outlined in Table 6, the stiffness ratios of the initial model were the same as the final damping-updated model for the undamaged caisson with HWL. For the damping parameters, experimental modal analysis of 'the damaged caisson with HWL' (ω_1=15.39 Hz, ω_2=42.24 Hz, ξ_1=12.08%, ξ_2=2.89%) were applied as the initial values to calculate the damping parameters.

The model update was performed in the same way as described previously. Table 6 outlines the calculated K and C matrices of the structural models in forms of relative values. Fig. 13 shows vibration responses of the initial model for the test case of "the damaged caisson with HWL". Fig. 14 shows vibration responses of the stiffness-updated model for the test case. Fig. 15 shows vibration responses of the damping-updated model for the test case. From the figures, it is observed that the two acceleration signals the two PSD curves become matched each other in the oscillating period, the peak frequencies and the dissipation slopes.

Table 7 outlines the estimated similarities of structural parameters of the updated models as compared to the experimental state of 'the undamaged caisson with LWL'. It is observed that the eigenvalue indices converge as stiffness updated and the RMSD indices converge as damping updated. Note that the convergence results verify the successful identification of the structural model corresponding to the foundation damage in the caisson system.

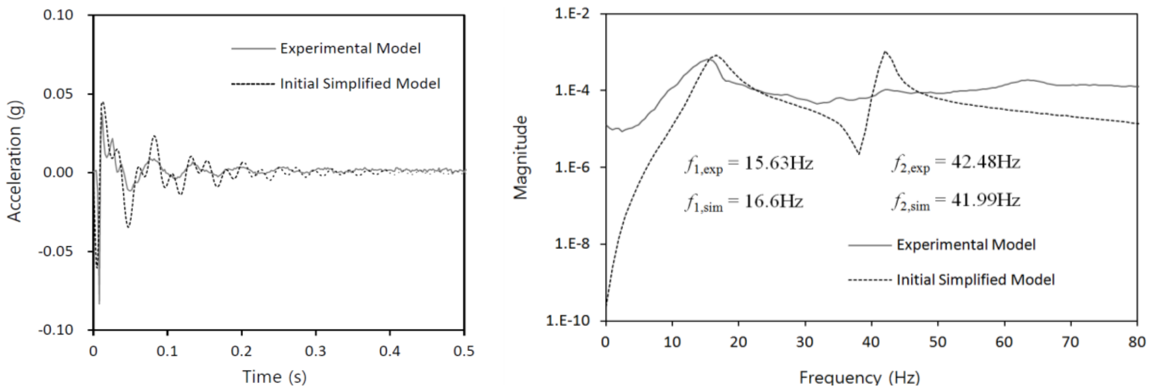

(a) Acceleration response (b) Power spectral density

Fig. 13 Vibration responses of initial model for 'the damaged caisson with HWL'

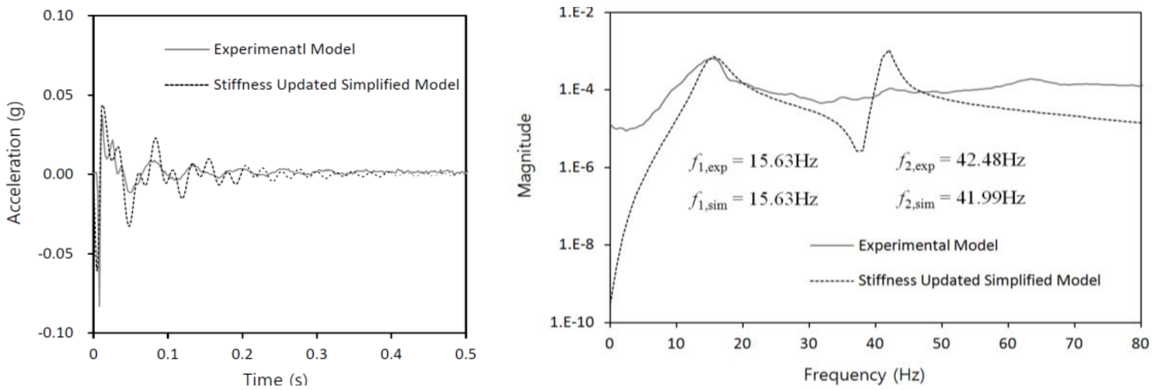

(a) Acceleration response (b) Power spectral density

Fig. 14 Vibration responses of stiffness-updated model for ‘the damaged caisson with HWL’

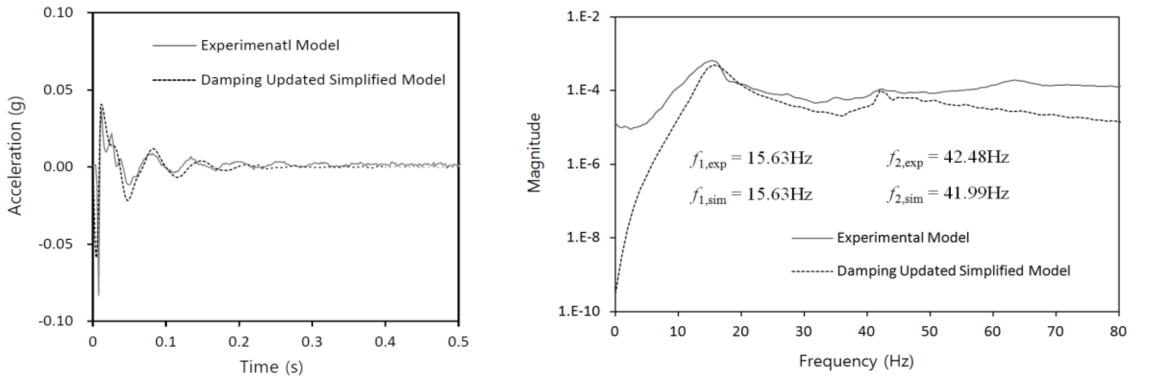

(a) Acceleration response (b) Power spectral density

Fig. 15 Vibration responses of damping-updated model for ‘the damaged caisson with HWL’

Table 6 Estimated structural parameters for ‘the damaged caisson with HWL’

	Stiffness ratio	K matrix	C matrix
Initial	$k_{S1} = k_{S4} = 1.5k_{F1}$ $k_{S2} = k_{S3} = 0.8k_{F2}$	$\begin{bmatrix} 1.21 & -0.80 & 0 \\ -0.80 & 2.60 & -0.80 \\ 0 & -0.80 & 1.21 \end{bmatrix} \times 10^6$	$\begin{bmatrix} 0.42 & 0.15 & 0 \\ 0.15 & 3.4 & 0.15 \\ 0 & 0.15 & 0.42 \end{bmatrix} \times 10^3$
Stiffness updated	$k_{S1} = k_{S4} = 1.22k_{F1}$ $k_{S2} = k_{S3} = 0.73k_{F2}$	$\begin{bmatrix} 1.31 & -0.90 & 0 \\ -0.90 & 2.80 & -0.90 \\ 0 & -0.90 & 1.31 \end{bmatrix} \times 10^6$	$\begin{bmatrix} 0.41 & 0.17 & 0 \\ 0.17 & 3.40 & 0.17 \\ 0 & 0.17 & 0.4 \end{bmatrix} \times 10^3$
Damping updated	$k_{S1} = k_{S4} = 1.22k_{F1}$ $k_{S2} = k_{S3} = 0.73k_{F2}$	$\begin{bmatrix} 1.31 & -0.90 & 0 \\ -0.90 & 2.80 & -0.90 \\ 0 & -0.90 & 1.31 \end{bmatrix} \times 10^6$	$\begin{bmatrix} 1.53 & -0.68 & 0 \\ -0.68 & 5.14 & -0.68 \\ 0 & -0.68 & 1.53 \end{bmatrix} \times 10^3$

Table 7 Convergence of structural models to 'the damaged caisson with HWL'

	Eigenvalue index		RMSD index	
	Mode 1	Mode 2	Mode 1	Mode 2
Initial	-0.1135	0.0235	0.0742	0.1110
Stiffness update	0.0	0.0235	0.0366	0.1141
Damping update	0.0	0.0235	0.0396	0.0494

As the foundation damage was simulated by 18.7% loss out of the bottom area (see Fig. 3), natural frequencies were decreased and damping coefficients were increased as outlined in Table 1. The updated structural model for the reference structure (Table 2) was compared to the corresponding one for the foundation-damaged state (Table 6). It is observed that system stiffness slightly decreased and system damping slightly increased due to the foundation damage.

6. Conclusions

A vibration-based structural identification method was proposed for the integrity assessment of gravity-type caisson structures. A simplified structural model with a few degrees-of-freedom (DOFs) was formulated to represent the gravity-type caisson structure that corresponds to the sensors' DOFs. Next, a structural identification algorithm based on the use of vibration characteristics of the limited DOFs was formulated to fine-tune stiffness and damping parameters of the structural model. At last, the experimental evaluation was performed on a lab-scaled gravity-type caisson structure in a 2-D wave flume.

For structural identification of the caisson structure, structural models were sequentially updated in three levels; i.e., initial, stiffness-updated, and damping-updated models. The stiffness-updated model's identification was successful in natural frequencies but different in damping properties as compared to the experimental state. Also, the damping-updated model's identification was successful both in natural frequencies and damping properties.

As the water level was decreased by 13% into low water-level, two major results were analyzed from vibration tests and structural identification as follows: first, natural frequencies were increased and damping coefficients were slightly decreased due to the water height decrement; and next, system stiffness slightly increased and system damping slightly decreased due to the water height decrement. As the foundation damage was simulated by 18.7% loss out of the bottom area of the foundation mound, two major results were analyzed as follows: first, natural frequencies were decreased and damping coefficients were increased due to the occurrence of damage; and next, system stiffness slightly decreased and system damping slightly increased due to the foundation damage.

Acknowledgements

This work was supported by Basic Science Research Program through the National Research

Foundation of Korea (NRF) funded by the Ministry of Education, Science and Technology (NFR-2013R1A1A2A10012040). The authors also would like to acknowledge the financial support of the project 'Development of inspection equipment technology for harbor facilities' funded by Korea Ministry of Land, Transportation, and Maritime Affairs.

References

Adams, R.D., Cawley, P, Pye, C.J. and Stone, B.J. (1978), "A vibration technique for non-destructively assessing the integrity of structures", *J. Mech. Eng. Sci.*, **20**(2), 93-100.

Aktan, A.E., Farhey, D.N., Helmicki, A.J., Brown, D.L., Hunt, V.J., Lee, K.L. and Levi, A. (1997), "Structural identification for condition assessment: experimental arts", *J. Struct. Eng. - ASCE*, **123**(12), 1674-1684.

Bowles, J.E. (1996), *Foundation Analysis and Desig*, (5th Ed.), McGraw-Hill.

Brinker, R., Zhang, L. and Andersen, P. (2001), "Modal identification of output-only systems using frequency domain decomposition", *Smart Mater. Struct.*, **10**(3), 441-445.

Ewins, D.J. (2000), *Modal Testing: theory, practice and application*, 2nd Ed., Research Studies Press LTD.

Goda, Y. (1994), "Dynamic response of upright breakwater to impulsive force of breaking waves", *Coastal Eng.*, **22**(1-2), 135-158.

Gul, M., Dumlupinar, T., Hattori, H. and Catbas, N. (2014), "Structural monitoring of movable bridge mechanical components for maintenance decision-making", *Struct. Monit. Maint.*, **1**(3), 249-271.

Huang, C. and Lee, S.Y. (2014), "Experimental study on bridge structural health monitoring using blind source separation method: arch bridge", *Struct. Monit. Maint.*, **1**(1), 69-87.

Huynh, T.C., Lee, S.Y., Kim, J.T., Park, W.S. and Han, S.H. (2013), "Simplified planar model for damage estimation of interlocked caisson system", *Smart Struct. Syst.*, **12**(3-4), 441-463.

Jang, S., Li, J. and Spencer, B.F., Jr (2012), "Corrosion estimation of a historic truss bridge using model updating", *J. Bridge Eng. - ASCE*, **18**(7), 678-689.

Kim, D.K., Ryu, H.R., Seo, H.R. and Chang, S.K. (2005), "Earthquake response characteristics of port structure according to exciting frequency components of earthquakes", *J. Korean Soc. Coastal Ocean Eng.*, **17**(1), 41-46.

Kim, J.T., Y.S. Ryu, Cho, H.M. and Stubbs, N. (2003), "Damage identification in beam-type structures: frequency-based method vs mode-shape-based method", *Eng. Struct.*, **25**, 57-67.

Lee, S.Y., Lee, S.R. and Kim, J.T. (2011), "Vibration-based structural health monitoring of harbor caisson structure", *Proc. of SPIE*, USA.

Lee, S.Y., Nguyen, K.D., Huynh, T.C., Kim, J.T., Yi, J.H. and Han, S.H. (2012), "Vibration-based damage monitoring of harbor caisson structure with damaged foundation-structure interface", *Smart Struct. Syst.*, **10**(6), 517-547.

Lee, S.Y., Huynh, T.C., Kim, J.T., Yoon, H.S. and Han, S.H. (2013), "Vibration characteristics of gravity-type caisson breakwater structure with water-level variation", *Int. J. Distrib. Sens. N.*, **2013** Article ID 261693, 10pages.

Lee, S.Y., Kim, J.T., Yi, J.H. and Kang, Y.K. (2009), "Structural health monitoring of harbor caisson-type structures using harmony search method", *J. Ocean Eng. Technol.*, **23**(1), 122-128.

Li, D.S., Li, H.N., Ren, L., Sun, L. and Zhou, J. (2004), "Experiments on an offshore platform model by FBG sensors", *Proc. of SPIE*, **5391**, 100-106.

Li, H.L., Yi, T.H., Ren, L., Li, D.S. and Huo, L.S. (2014), "Reviews on innovations and applications in structural health monitoring for infrastructures", *Struct. Monit. Maint.*, **1**(1), 1-45.

Marinski, J.G. and Oumeraci, H. (1992), "Dynamic response of vertical structures to breaking wave forces – review of the CIS design experience", *Proceedings of the 23rd Int. Conf. Coastal Eng., Venice*, ASCE, New York.

Ming, G., Guanying, D. and Jihua, Y. (1988), "Dynamic studies on caisson-type breakwaters", *Proc. Coastal*

Eng., 2469-2478.
Oumeraci, H. and Kortenhaus, A. (1994), "Analysis of the dynamic response of caisson breakwaters", *Coastal Eng.*, **22**(1-2), 159-183.
Smirnov, G.N. and Moroz, L.R. (1983), "Oscillations of gravity protective structures of a vertical wall type", *Proceedings of the IAHR, 20th Congress*.
Stubbs, N. and Osegueda, R. (1990), "Global non-destructive damage evaluation in solids", *Int. J. Anal. Exper. Modal*, **5**(2), 67-79.
Takahashi, S., Shimosako, K., Kimura, K. and Suzuki, K. (2000), "Typical failure of composite breakwaters in Japan", *Proceedings of the 27th International Conference on Coastal Engineering*.
Vink, H.A.Th. (1997), *Wave Impacts on Vertical Breakwaters*, Master's thesis, Faculty of Civil Engineering, Delft University of Technology, The Netherlands.
Wang, Y.Z., Zhu, Z.W. and Dong, S.W. (2006), "A probabilistic method for motion analysis of caisson breakwaters", *China Ocean Eng*., **20**(1), 73-84.
Westergaard, H.M. (1933), "Water pressures on dams during earthquakes", *T. Am. Soc.*, **98**(2), 418-432.
Wilson, E.L. (2004), *Static and Dynamic Analysis of Structures*, (4th Ed.), Berkeley, CA: Computers and Structures, Inc.
Yang, Z., Elgamal, A., Abdoun, T. and Lee, C.J. (2001), "A numerical study of lateral spreading Behind a caisson-type quay wall", *Proceedings of the 4th International Conference on Recent Advances in Geotechnical Earthquake Engineering and Soil Dynamics and Symposium*, San Diego.
Yi, J.H., Park, W.S., Lee, S.Y., Huynh, T.C., Kim, J.T. and Seo, C.G. (2013), "Evaluation of vibration characteristics of existing harbor caisson structure using tugboat impact tests and modal analysis", *Int. J. Distrib. Sens. N.*, **2013**, Article ID 806482, 11pages.
Yi, J.H. and Yun, C.B (2004), "Comparative study on modal identification methods using output-only information", *Struct. Eng. Mech.- ASCE*, **17**(3-4), 445-456.
Yoon, H.S., Lee, S.Y., Kim, J.T. and Yi, J.H. (2012), "Field Implementation of Wireless Vibration Sensing System for Monitoring of Harbor Caisson Breakwaters", *Int. J. Distrib. Sens. N.*, **2012**, 1-9.
You, T., Gardoni, P. and Hurlebaus, S. (2014), "Iterative damage index method for structural health monitoring", *Struct. Monit. Maint.*, **1**(1), 89-110.
Yun G.J., Ogorzalek, K.A., Dyke, S.J. and Song, W. (2009), "A two-stage damage detection approach based on subset of damage parameters and genetic algorithms", *Smart Struct. Syst.*, **5**(1), 1-21.
Zhang, X.Y. (2006), *Behaviour of caisson breakwater subjected to breaking waves*, Dissertation, National university of Singapore.